Parton degrees of freedom from the path-integral formalism

Keh-Fei Liu
National Center for Theoretical Sciences, P.O. Box 2-131, Hsinchu, Taiwan 300
and Department of Physics and Astronomy, University of Kentucky, Lexington, Kentucky 40506
(Received 14 October 1999; published 22 August 2000)

We formulate the hadronic tensor $W_{\mu\nu}$ of deep inelastic scattering in the path-integral formalism. It is shown that there are 3 gauge invariant and topologically distinct contributions. In addition to the valence contribution, there are two sources for the sea—one in the connected insertion and the other in the disconnected insertion. The operator product expansion is carried out in this formalism. The operator rescaling and mixing reveal that the connected sea partons evolve the same way as the valence; i.e., their evolution is decoupled from the disconnected sea and the gluon distribution functions. We explore the phenomenological consequences of this classification in terms of the small x behavior, Gottfried sum rule violation, and flavor dependence. In particular, we point out that in the nucleon $\bar{u}$ and $\bar{d}$ partons have both connected and disconnected sea contributions, whereas the $\bar{s}$ parton has only the disconnected sea contribution. This difference between $\bar{u}+\bar{d}$ and $\bar{s}$, as far as we know, has not been taken into account in the fitting of parton distribution functions to experiments.

PACS number(s): 11.15.Ha, 13.60.Hb

I. INTRODUCTION

In the past decade, the surprising results of a small quark spin content (flavor-singlet g_A^0) [1] and the discovery that $\bar{u} \neq \bar{d}$ in the nucleon [2] from deep inelastic scattering have focused people's attention on the interplay between the parton model at high energies and the hadronic structure at low energies. The connection is often made through the operator product expansion which relates the sum rules of parton distribution functions to the forward matrix elements. The latter can be obtained from low energy experiments.

In the parton model, the dynamical quark degrees of freedom are taken to be the valence and the sea, whereas in the hadronic models the degrees of freedom involve the valence and the meson cloud. The classification of these dynamical degrees of freedom in deep inelastic scattering has been made in the path integral formalism [3,4]. It is revealed that there are two sources for the sea quark. One is in the connected insertion and the other in the disconnected insertion. Their relations to the meson cloud in the hadronic models for hadrons near the rest frame and chiral symmetry have been clarified and extensively explored in the context of hadronic models in terms of the form factors, hadron masses, and matrix elements, i.e. low-energy quantities which can be calculated in the two- and three-point functions. In addition, it is shown that when both the connected sea (referred to as cloud in Ref. [4]) and the disconnected sea quarks are eliminated in a valence QCD theory, the valence quark picture with SU(6) symmetry emerges. In this paper, we shall derive the operator product expansion in the path-integral formalism and explore the phenomenological consequences of this classification of the parton degrees of freedom. Section II is on the path-integral formalism of the hadronic tensor and the classification of the parton degrees of freedom. Section III shows how to carry out the operator product expansion in the path-integral formalism and to derive parton evolution equations through operator rescaling and mixing. Section IV explores the phenomenological consequences. We shall show that the small x behavior of the connected sea is different from that of the disconnected sea and the violation of the Gottfried sum rule, i.e., $\bar{u} \neq \bar{d}$, comes only from the connected sea at the flavor $SU(2)$ limit. Finally, we emphasize that $\bar{u}+\bar{d}$ in the nucleon has both the connected sea and the disconnected sea contributions, whereas $\bar{s}$ has only the disconnected sea contribution. This difference has not been parametrized in extracting the parton distribution functions from the experiments. The conclusion is given in Sec. V.

II. PATH-INTEGRAL FORMALISM

The deep inelastic scattering of a muon on a nucleon involves the hadronic tensor which, being an inclusive reaction, involves all intermediate states

$$W_{\mu\nu}(q^2,\nu) = \frac{1}{2M_N} \sum_n (2\pi)^3 \delta^4(p_n - p - q) \langle N|J_\mu(0)|n\rangle \times \langle n|J_\nu(0)|N\rangle_{spin\ ave.}. \tag{1}$$

Since deep inelastic scattering measures the absorptive part of the Compton scattering, it is the imaginary part of the forward amplitude and can be expressed as the current-current correlation function in the nucleon: i.e.,

$$W_{\mu\nu}(q^2,\nu) = \frac{1}{\pi} \mathrm{Im}\, T_{\mu\nu}(q^2,\nu) = \frac{1}{2M_N} \left\langle N \left| \int \frac{d^4x}{2\pi} e^{iq\cdot x} J_\mu(x) J_\nu(0) \right| N \right\rangle_{spin\ ave.}. \tag{2}$$

It has been shown [3,4] that the hadronic tensor $W_{\mu\nu}(q^2,\nu)$ can be obtained from the Euclidean path-integral formalism where the various parton dynamical degrees of freedom are readily and explicitly revealed. In this case, one considers the ratio of the four-point function

$(2E_pV/2M_N)\langle O_N(t)\int(d^3x/2\pi)e^{-i\vec{q}\cdot\vec{x}}J_\mu(\vec{x},t_2)J_\nu(0,t_1)O_N(0)\rangle$ and the two-point function $\langle O_N[t-(t_2-t_1)]O_N(0)\rangle$, where $O_N(t)$ is an interpolation field for the nucleon with momentum p at Euclidean time t.

As both $t-t_2\gg 1/\Delta E_p$ and $t_1\gg 1/\Delta E_p$, where ΔE_p is the energy gap between the nucleon energy E_p and the next excitation (i.e., the threshold of a nucleon and a pion in the p-wave), the intermediate state contributions will be dominated by the nucleon with the Euclidean propagator $e^{-E_p[t-(t_2-t_1)]}$. Hence,

$$\begin{aligned}\tilde{W}_{\mu\nu}(\vec{q}^2,\tau)&=\left.\frac{\frac{2E_pV}{2M_N}\left\langle O_N(t)\int\frac{d^3x}{2\pi}e^{-i\vec{q}\cdot\vec{x}}J_\mu(\vec{x},t_2)J_\nu(0,t_1)O_N(0)\right\rangle}{\langle O_N(t-\tau)O_N(0)\rangle}\right|_{\substack{t-t_2\gg 1/\Delta E_p\\ t_1\gg 1/\Delta E_p}}\\ &=\frac{\frac{f^2 2E_pV}{2M_N}e^{-E_p(t-t_2)}\left\langle N\left|\int\frac{d^3x}{2\pi}e^{-i\vec{q}\cdot\vec{x}}J_\mu(\vec{x},t_2)J_\nu(0,t_1)\right|N\right\rangle e^{-E_pt_1}}{f^2e^{-E_p(t-\tau)}}\\ &=\frac{2E_p}{2M_N}\left\langle N\left|\int\frac{d^3x}{2\pi}e^{-i\vec{q}\cdot\vec{x}}J_\mu(\vec{x},t_2)J_\nu(0,t_1)\right|N\right\rangle,\end{aligned}\tag{3}$$

where $\tau=t_2-t_1$ and f is the transition matrix element $\langle 0|O_N|N\rangle$, and V is the 3-volume. Inserting intermediate states, $\tilde{W}_{\mu\nu}(\vec{q}^2,\tau)$ becomes

$$\tilde{W}_{\mu\nu}(\vec{q}^2,\tau)=\frac{1}{2M_N}\sum_n(2\pi)^2\delta^3(p_n-p+q)\langle N|J_\mu(0)|n\rangle\times\langle n|J_\nu(0)|N\rangle_{spin\ ave.}e^{-(E_n-E_p)\tau}.\tag{4}$$

To go back to the delta function $\delta(E_n-E_p+\nu)$ in Eq. (1), one needs to carry out the inverse Laplace transform [5,3]

$$W_{\mu\nu}(q^2,\nu)=\frac{1}{i}\int_{c-i\infty}^{c+i\infty}d\tau e^{\nu\tau}\tilde{W}_{\mu\nu}(\vec{q}^2,\tau),\tag{5}$$

with $c>0$. This is basically doing the anti-Wick rotation back to the Minkowski space.

In the Euclidean path-integral formulation of $\tilde{W}_{\mu\nu}(\vec{q}^2,\tau)$ in Eq. (4), contributions to the four-point function can be classified according to different topologies of the quark paths between the source and the sink of the proton. They represent different ways the fields in the currents J_μ and J_ν contract with those in the nucleon interpolation operator O_N. Figures 1(a) and 1(b) represent connected insertions (CI) of the currents. Here the quark fields from the interpolators O_N contract with the currents such that the quark lines flow continuously from $t=0$ to $t=t$. Figure 1(c), on the other hand, represents a disconnected insertion (DI) where the quark fields from J_μ and J_ν self-contract and are hence disconnected from the quark paths between the proton source and sink. Here, ''disconnected'' refers only to the quark lines. Of course, quarks dive in the background of the gauge field and all quark paths are ultimately connected through the gluon field.

Figure 1 represents the contributions of the class of ''handbag'' diagrams where the two currents are hooked on the same quark line. These contain leading twist contributions in deep inelastic scattering. Other contractions with the two currents hooking on different quark lines involve only higher twist operators and thus will be suppressed in the Bjorken limit [4]. They are shown in Fig. 2. We will neglect these ''cat's ears'' diagrams from now on. We should stress that these diagrams in Figs. 1 and 2 are *not* Feynman diagrams to repesent the forward Compton scattering amplitude $T_{\mu\nu}(q^2,\nu)$ and should not be read as such. Rather, they are path-integral diagrams needed to formulate $W_{\mu\nu}(q^2,\nu)$ which is the imaginary part of $T_{\mu\nu}(q^2,\nu)$ [see Eq. (2)] or its s-channel discontinuity.

In the deep inelastic limit, the Bjorken scaling implies that the current product (or commutator) is dominated by the light-cone singularity of a free-field theory, i.e., $1/x^2$ where $x^2\approx O(1/Q^2)$. Among the time-fixed diagrams in Fig. 1, Fig. 1(a)/1(b) involves only a quark/antiquark propagator between the currents; whereas, Fig. 1(c) has both quark and antiquark propagators. Hence, there are two distinct classes of diagrams where the sea quarks contribute. One comes from the DI; the other comes from the CI. It is usually assumed that connected insertions involve only ''valence'' quarks which are responsible for the baryon number. This is obviously not true, there are also quark-antiquark pairs in the

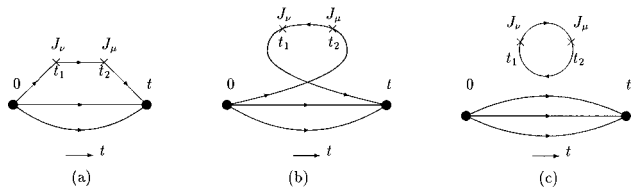

FIG. 1. Quark skeleton diagrams in the Euclidean path integral formalism for evaluating $W_{\mu\nu}$ from the four-point function defined in Eq. (3). These include the lowest twist contributions to $W_{\mu\nu}$. (a) and (b) are connected insertions and (c) is a disconnected insertion.

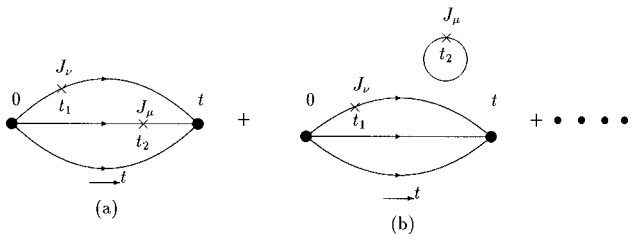

FIG. 2. Quark skeleton diagrams similar to those in Fig. 1, except that the two current insertions are on different quark lines. They give higher twist contributions to $W_{\mu\nu}$.

CI. To define the quark distribution functions more precisely, we shall call the quark/antiquark distribution from the DI (which are connected to the ''valence'' quark propagators and other quark loops through gluons) the ''disconnected sea'' quark/antiquark. We shall refer to the antiquark in the backward time going quark propagator between t_1 and t_2 in Fig. 1(b) as the ''connected sea'' antiquark. On the other hand, the quark in the time forward propagator between t_2 and t_1 in Fig. 1(a) includes both the valence and the ''connected sea'' quarks. This is because a quark propagator from $t=0$ to $t=t(t>0)$ involves both the time forward and backward zigzag motions so that one cannot tell if the quark propagator between t_2 and t_1 is due to the valence or the connected sea. All one knows is that it is a quark propagator. In other words, one needs to consider connected sea quarks in addition to the valence in order to account for the production of quark-antiquark pairs in a connected fashion [Fig. 1(a)]; whereas, the pair production in a disconnected fashion is in Fig. 1(c).

We should stress that this separation into three topologically distinct classes of path-integral diagrams is gauge invariant. Notice that all the quark propagators are sewed together in a trace over color. In a perturbative illustration of the distinction between Fig. 1(b) and Fig. 1(c), one may consider the time-ordered perturbation where Fig. 1(c) represents the vacuum polarization contribution as a disconnected insertion in a direct diagram. The corresponding exchange diagram where the quark in the loop in Fig. 1(c) is exchanged with one in the ''valence'' will lead to a connected insertion which falls in the class of Fig. 1(b) [3,6]. However, the separation depends on the momentum frame of the nucleon, although the sum which corresponds to the full physical $W_{\mu\nu}(q^2,\nu)$ does not. For example, when the quark/antiquark propagator between the currents is either from the nucleon interpolation field or pair-produced before the current J_ν at t_1, i.e., it is preexisting in the wave function, then it is not suppressed in the large momentum frame. Whereas, if it is pair-produced by the current J_ν, then it is suppressed by $|\vec{p}|^2$ where $|\vec{p}|$ is the momentum of the nucleon. This has been known since current algebra sum rules were studied at large $|\vec{p}|$ [7].

Since the parton model acquires its natural interpolation in the large momentum frame of the nucleon, i.e., $|\vec{p}|\geqslant|\vec{q}|$, the parton distribution is then defined via $\nu W_2(Q^2,\nu)\rightarrow F_2(x,Q^2)=x\Sigma_i e_i^2[q_i(x,Q^2)+\overline{q}_i(x,Q^2)]$ in the large momentum frame. Here x is the Bjorken scaling variable $x=Q^2/2m\nu$. Given the specific time-ordering in Fig. 1, Fig. 1(a)/1(b) involves only a quark/antiquark propagator between the currents; whereas, Fig. 1(c) has both quark and antiquark propagators. Consequently, the parton densities for the u and d antiquarks in the nucleon come from two sources, i.e. for the case of u,

$$\overline{u}(x,Q^2)=\overline{u}_{cs}(x,Q^2)+\overline{u}_{ds}(x,Q^2), \tag{6}$$

where $\overline{u}_{cs}(x,Q^2)$ is the ''connected sea'' (CS) u anti-parton distribution from the CI in Fig. 1(b) and $\overline{u}_{ds}(x,Q^2)$ denotes the ''disconnected sea'' (DS) u antiparton distribution from the DI in Fig. 1(c). Similarly, $\overline{d}$ has two components. The strange and charm partons, on the other hand, only appear in the DI in Fig. 1(c). Thus,

$$\overline{s}(x,Q^2)\equiv\overline{s}_{ds}(x,Q^2). \tag{7}$$

One can prove Eq. (7) this way. First, it is imperative to note that the hardronic tensor $\tilde{W}_{\mu\nu}(\vec{q}^2,\tau)$ in Eq. (3) does not depend on the specific form of the interpolation field, except its quantum numbers. In fact, the interpolation-field dependent transition matrix element $f=\langle 0|O_N|N\rangle$ drops out in the ratio of the four-point to two-point functions in Eq. (3). As such, one can use the simplest interpretation field of the nucleon which involves only the valence quark field. For example, $O_N(t)$ can be taken to be the two u and one d quark fields with nucleon quantum numbers,

$$O_N=\int d^3x e^{i\vec{p}\cdot\vec{x}}\varepsilon^{abc}\Psi^{(u)a}(x)([\Psi^{(u)b}(x)]^T C\gamma_5\Psi^{(d)c}(x)), \tag{8}$$

for the proton. Since the interpolation field O_N does not involve strange quarks, the strange parton contribution can only come from the vacuum polarization due to the external currents J_μ and J_ν, in other words, the DI in Fig. 1(c). As a corollary, one can also prove it for the case if one uses the $O_N s\overline{s}$ as the interpolation field, for example. In this case, there are two classes of path-integral diagrams. One class involves the CI where the strange quark fields in the currents $\overline{s}\gamma_\mu s$ and $\overline{s}\gamma_\nu s$ contract with those strange quark fields in the interpolation field $O_N s\overline{s}$ for the nucleon source and sink. This class of diagrams does not project to the nucleon as its lowest mass state, since the physical states it projects to will involve 5 valence quarks, i.e., $uuds\overline{s}$. Instead, it will project to states such as the nucleon and a scalar $s\overline{s}$ meson. Since they all have masses higher than the nucleon, they will be exponentially suppressed relative to the nucleon as the time separation $t-t_2$ and t_1 in Eq. (3) are large. The other class involves a DI where the strange quark fields in the nucleon source and sink self contract, so are the strange quark fields in the currents. This will project to the nucleon state with uud as the valence quarks. Since the transition matrix element $f=\langle 0|O_N s\overline{s}|N\rangle$ is divided out in the ratio in Eq. (3), it yields the same result as that obtained with O_N as the interpolation field. Thus, in either case, the strange parton contribution comes only from the DI in Fig. 1(c).

Similarly, the u and d partons have 2 sources, i.e.,

$$u(x,Q^2)=u_{v+cs}(x,Q^2)+u_{ds}(x,Q^2), \tag{9}$$

where $u_{v+cs}(x,Q^2)$ denotes the valence and CS u partons and $u_{ds}(x,Q^2)$ denotes the DS u parton and they are from Fig. 1(a) and Fig. 1(c), respectively. Again these two components applies to the d partons; whereas, the s parton has only the DS component.

III. OPERATOR PRODUCT EXPANSION (OPE)

In the Minkowski space, the operator product expansion (OPE) is carried out in the unphysical region of $T_{\mu\nu}$ which is defined with the time-ordered product of the currents. How does one carry this out in the Euclidean path-integral formulation? It turns out that because $\tilde{W}_{\mu\nu}(\vec{q}^2,\tau)$ is defined in the Euclidean path-integral [Eq. (4)], it requires several steps to get to $T_{\mu\nu}$ in the Minkowski space. On the other hand, it is relatively easy to do so because it entails a simple Taylor expansion of functions as opposed to dealing with operators in the usual OPE, as we shall see.

Considering Fig. 1(a) first, the three-point function in Eq. (3) involves the following expression:

$$\begin{aligned}\tilde{W}_{\mu\nu}(\vec{q}^2,\tau)\propto&\int d[A]\det M(A)e^{-S_g}\\&\times\mathrm{Tr}\Big[\cdots M^{-1}(t,t_2)\int d^3x e^{-i\vec{q}\cdot\vec{x}}i\gamma_\mu\\&\times M^{-1}(t_2,t_2-\tau)i\gamma_\nu M^{-1}(t_2-\tau,0)\cdots\Big],\end{aligned} \tag{10}$$

where S_g is the action for the gluon field A, M^{-1} is the quark propagator with arguments labeled by the Euclidean time. The spatial indices are implicit and have been integrated over to give the nucleon a definite momentum $|\vec{p}|$ and a momentum transfer $\vec{q}$. $\vec{x}$ and τ are the spatial and time separations of the two currents J_μ and J_ν. The trace is over the color and spin indices. The expression in Eq. (10) exhibits the part of the result from the quark line on which the currents are attached. The other two quark propagators and the nucleon interpolation field operators are indicated by the dots.

Similar to the usual OPE derivation [8], we shall consider the most singular part of the quark propagator between the currents in Fig. 1. In the deep inelastic scattering (DIS) limit where both the momentum transfer $|\vec{q}|$ and energy transfer $\nu\to\infty$, the leading singularity comes from the short-distance part in $\tilde{W}_{\mu\nu}(\vec{q}^2,\tau)$ where $|\vec{x}|$ and $\tau\to 0$. Therefore, we replace the quark propagator between the currents with the free massless propagator

$$M^{-1}(t_2,t_2-\tau)\to\frac{1}{4\pi^2}\frac{\not{b}}{\vec{x}^2+\tau^2}. \tag{11}$$

We also carry out the Taylor expansion of the propagator $M^{-1}(t_2-\tau,0)$ for small τ and $\vec{x}$

$$M^{-1}(t_2-\tau,0)=e^{\vec{x}\cdot\vec{D}+\tau D_\tau}M^{-1}(t_2,0), \tag{12}$$

where D is the covariant derivative. With these substitutions, the corresponding hadronic tensor $W_{\mu\nu}(q^2,\nu)$ from Fig. 1(a) after the Fourier transform in space and Laplace transform in τ [Eq. (5)] is given as

$$\begin{aligned}W_{\mu\nu}(q^2,\nu)\propto\mathrm{Tr}\Big[&\cdots M^{-1}(t,t_2)i\gamma_\mu\frac{-i\pi(\not{q}+i\not{D})}{|\vec{q}+i\vec{D}|}\\&\times\delta(\nu+D_\tau-|\vec{q}+i\vec{D}|)i\gamma_\nu M^{-1}(t_2,0)\cdots\Big].\end{aligned} \tag{13}$$

Since $W_{\mu\nu}(q^2,\nu)$ is the imaginary part of $T_{\mu\nu}$, i.e., $W_{\mu\nu}(q^2,\nu)=(1/\pi)\mathrm{Im}\,T_{\mu\nu}(q^2,\nu)$, one can use the dispersion relation to obtain $T_{\mu\nu}$ from $W_{\mu\nu}$,

$$\begin{aligned}T_{\mu\nu}(q^2,\nu)=&\frac{1}{\pi}\int_{Q^2/2M_N+D_\tau}^{\infty}d\nu'\frac{\nu' W_{\mu\nu}(q^2,\nu'-D_\tau)}{\nu'^2-(\nu+D_\tau)^2},\\\propto&\mathrm{Tr}\Big[\cdots M^{-1}(t,t_2)i\gamma_\mu\frac{-i(\not{q}+i\not{D})}{Q^2+2iq\cdot D-D^2}i\gamma_\nu\\&\times M^{-1}(t_2,0)\cdots\Big],\end{aligned} \tag{14}$$

where we have used $\tau=it$ and $D_t=iD_\tau$ so that $D=(\vec{D},-iD_t)$ is the covariant derivative in Minkowski space. Expanding $T_{\mu\nu}$ in the unphysical region where $-2p\cdot q/Q^2<1$, the expression between the γ's in Eq. (14) gives

$$\frac{-i(\not{q}+i\not{D})}{Q^2+2iq\cdot D-D^2}=\frac{-i(\not{q}+i\not{D})}{Q^2}\sum_{n=0}^{\infty}\left(\frac{-2iq\cdot D+D^2}{Q^2}\right)^n. \tag{15}$$

From this we obtain the valence and CS parton leading twist contributions to $T_{\mu\nu}$ from Fig. 1(a)

$$\begin{aligned}T_{\mu\nu}(q_{v+cs})=\sum_f e_f^2\Big[&8p_\mu p_\nu\sum_{n=2}\frac{(-2q\cdot p)^{n-2}}{(Q^2)^{n-1}}A_f^n(\mathrm{CI})\\&-2\delta_{\mu\nu}\sum_{n=2}\frac{(-2q\cdot p)^n}{(Q^2)^n}A_f^n(\mathrm{CI})\Big]+\cdots,\end{aligned} \tag{16}$$

where f indicates flavor. For the nucleon, it only involves u and d in the CI. $A_f^n(\mathrm{CI})$ is defined through the following consideration. We first note that the short-distance expansion in Eq. (15) leads $T_{\mu\nu}(q_{v+cs})$ to a series of terms represented by the three-point functions in Fig. 3(a) which correspond to matrix elements calculated through the CI expression

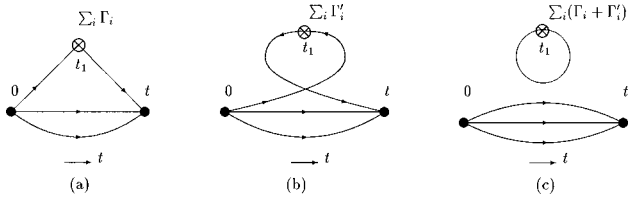

FIG. 3. Quark skeleton diagrams in the Euclidean path integral formalism considered in the evaluation of matrix elements for the sum of local operators from the operator product expansion of $J_\mu(x)J_\nu(0)$. (a), (b) and (c) correspond to the operator product expansion from Figs. 1(a), 1(b) and 1(c), respectively.

$$\int d[A]\det M(A)e^{-S_g}\mathrm{Tr}[\cdots M^{-1}(t,t_2)O_f^n M^{-1}(t_2,0)\cdots], \tag{17}$$

where the operator O_f^n is

$$O_f^n = i\gamma_{\mu 1}\left(\frac{-i}{2}\right)^{n-1}\vec{D}_{\mu 2}\vec{D}_{\mu 3}\ldots\vec{D}_{\mu n}. \tag{18}$$

The ratio of these three-point functions in Fig. 3(a) to the appropriate two-point functions then define the forward matrix element which in turn defines the coefficient $A_f^n(\mathrm{CI})$ in Eq. (16),

$$\langle p|\bar{\Psi}O_f^n\Psi|p\rangle_{\mathrm{CI}} = A_f^n(\mathrm{CI})2p_{\mu_1}p_{\mu_2}\ldots p_{\mu_n}. \tag{19}$$

Similarly, we can perform the short-distance expansion for the CS antiparton in Fig. 1(b) and obtain the same expression as in Eq. (16) except with the substitution $q\to -q$. As a result, this leads to the even n terms minus the odd n terms instead of the sum as in Eq. (16), i.e.,

$$T_{\mu\nu}(\overline{q}_{cs}) = \sum_{even=2}\cdots A_f^n(\mathrm{CI}) - \sum_{odd=3}\cdots A_f^n(\mathrm{CI}). \tag{20}$$

In other words, the short-distance expansion of $T_{\mu\nu}$ from Fig. 1(b) yields three-point functions with a series of insertion of the same operators $\bar{\Psi}O_f^n\Psi$ except with a minus sign for the odd n terms. This is illustrated in Fig. 3(b) where Γ_n' denotes the n-th term insertion with the operator O_f^n and the associated kinematic factors in Eq. (16). Comparing Γ_n' in Fig. 3(b) and the corresponding Γ_n in Fig. 3(a), the minus sign for the odd n terms in Eq. (20) implies that $\Gamma_n' = (-)^n\Gamma_n$.

By the same token, the short-distance expansion for the DS parton/antiparton contribution in $T_{\mu\nu}$ from Fig. 1(c) gives

$$T_{\mu\nu}(q_{ds}/\overline{q}_{ds}) = \sum_{even=2}\cdots A_f^n(\mathrm{DI}) + \Big/ - \sum_{odd=3}\cdots A_f^n(\mathrm{DI}). \tag{21}$$

They have the same expression as $T_{\mu\nu}(q_{v+cs})$ and $T_{\mu\nu}(\overline{q}_{cs})$ except $A_f^n(\mathrm{DI})$ are from the DI part of the matrix element

$$\langle p|\bar{\Psi}O_f^n\Psi|p\rangle_{\mathrm{DI}} = A_f^n(\mathrm{DI})2p_{\mu_1}p_{\mu_2}\ldots p_{\mu_n}. \tag{22}$$

In this case, the leading twist expansion of the DS contribution to $T_{\mu\nu}$ in Fig. 1(c) now leads to two series of forward matrix elements of DI. One is for $T_{\mu\nu}(q_{ds})$ with even plus odd n terms; the other is $T_{\mu\nu}(\overline{q}_{ds})$ with even minus odd n terms as given in Eq. (21). Both are represented in the three-point functions in Fig. 3(c). It is worth pointing out that $T_{\mu\nu}(q_{v+cs})$ in Eq. (16) and $T_{\mu\nu}(q_{ds})$ in Eq. (21) are the same as those derived from the contraction of the inner pair of the quark fields in the conventional operator product expansion of the time-ordered current-current product $\overline{q}(x)\gamma_\mu q(x)\overline{q}(0)\gamma_\nu q(0)$ [8]. On the other hand, $T_{\mu\nu}(\overline{q}_{cs})$ in Eq. (20) and $T_{\mu\nu}(\overline{q}_{ds})$ in Eq. (21) are the same as those from the contraction of the outer pair of the quark fields in the current-current product. The only difference is that the path-integral formalism allows the separation into the CI and the DI.

When the parts in Eqs. (16), (20), and (21) are summed up, only the even n terms of the OPE are left

$$\begin{aligned} T_{\mu\nu} &= T_{\mu\nu}(q_{v+cs}) + T_{\mu\nu}(\overline{q}_{cs}) + T_{\mu\nu}(q_{ds}+\overline{q}_{ds}) \\ &= 2\sum_{n=2,even}\cdots[A_f^n(\mathrm{CI}) + A_f^n(\mathrm{DI})]. \end{aligned} \tag{23}$$

This is the same as derived from the ordinary OPE. However, what is achieved with the path-integral formulation is the separation of CI from DI in addition to the separation of partons from antipartons. This has not been possible with other formulations, e.g. the light-cone definition of the distribution function. This separation facilitates the derivation of the different small x behavior between the CS and the DS, the identification of the CS parton as the source of the Gottfried sum rule violation, and a different evolution of $\overline{q}_{cs}(x,Q^2)$ from that of $q_{ds}(x,Q^2)$ and $\overline{q}_{ds}(x,Q^2)$ as we shall see.

Now consider the contour integral of T_2 in the CI and DI parts of $T_{\mu\nu}$ around $\nu=0$ in the complex ν plane while keeping Q^2 fixed. $\oint(d\nu/2\pi i)[T_2(\nu,Q^2)/\nu^{n-1}]$ picks up the ν^{n-2} term in the series expansion of T_2 in Eqs. (16), (20), and (21) (N.B. $-2q\cdot p = 2M_p\nu$ in these equations.)

$$\oint\frac{d\nu 2M_p}{2\pi i}\frac{T_2(\nu,Q^2)}{\nu^{n-1}} = \sum_f 8e_f^2\left(\frac{2M_p}{Q^2}\right)^{n-1}A_f^n, \tag{24}$$

for both the CI and the DI. The contour of the integral can be distorted to turn the above integral into an integral over the discontinuities of T_2. Through the dispersion relation, this gives

$$\begin{aligned} &2\int_{Q^2}^{\infty}\frac{d\nu 2M_p}{2\pi i}\frac{2i\,\mathrm{Im}\,T_2(\nu,Q^2)}{\nu^{n-1}} \\ &\quad = 8\left(\frac{2M_p}{Q^2}\right)^{n-1}\int_0^1 dx x^{n-2}\frac{2M_p\nu W_2(\nu,Q^2)}{4}. \end{aligned} \tag{25}$$

Equating these two integrals and relating W_2 to the parton distribution function, one obtains the moment sum rules. Since $T_2(Q^2,\nu)$ is symmetric with respect to $\nu\rightarrow-\nu$, we obtain only the sum rules for even n. Thus,

$$A_f^{n=even}(\mathrm{CI})=M^n(\mathrm{CI}) \equiv \int_0^1 dx\, x^{n-1}[q_{v+cs}(x,Q^2)+\overline{q}_{cs}(x,Q^2)],$$

$$A_f^{n=even}(\mathrm{DI})=M^n(\mathrm{DI}) \equiv \int_0^1 dx\, x^{n-1}[q_{ds}(x,Q^2)+\overline{q}_{ds}(x,Q^2)]. \tag{26}$$

Similarly we obtain the moment sum rules for the odd n from the W_3 form factor through the interference of the vector and axial vector currents,

$$A_f^{n=odd}(\mathrm{CI})=M^n(\mathrm{CI}) \equiv \int_0^1 dx\, x^{n-1}[q_{v+cs}(x,Q^2)-\overline{q}_{cs}(x,Q^2)],$$

$$A_f^{n=odd}(\mathrm{DI})=M^n(\mathrm{DI}) \equiv \int_0^1 dx\, x^{n-1}[q_{ds}(x,Q^2)-\overline{q}_{ds}(x,Q^2)]. \tag{27}$$

One can define the valence parton distribution

$$q_v(x,Q^2)\equiv q_{v+cs}(x,Q^2)-\overline{q}_{cs}(x,Q^2). \tag{28}$$

In this case, $A_f^{n=odd}$ gives the sum rules for the valence distribution. In particular, valence number sum rules

$$M_u^1(\mathrm{CI})\equiv\int_0^1 dx\, u_v(x,Q^2)=2,$$

$$M_d^1(\mathrm{CI})\equiv\int_0^1 dx\, d_v(x,Q^2)=1,$$

$$M_f^1(\mathrm{DI})\equiv\int_0^1 dx[q_{ds}(x,Q^2)-\overline{q}_{ds}(x,Q^2)]=0, \tag{29}$$

for the u and d quarks in the proton reflect the charge conservation of the vector current $\Psi i\gamma_\mu\Psi$ and the fact that the DS carries no net charge.

We note that the matrix elements associated with $A_f^{n=even}(\mathrm{CI})$ include not just the valence but also the CS contribution. This is why the matrix element $A_{u,d}^2(\mathrm{CI})$, which corresponds to the momentum fraction $M^2(\mathrm{CI})=\langle x\rangle_{\mathrm{CI}}$, when calculated on the lattice [9,10], is larger than that obtained from the experiments for the valence partons only, i.e., $\langle x\rangle_{\mathrm{CI}}>\langle x\rangle_v$ at $\mu\sim 2$ GeV.

Operator rescaling and mixing, and parton evolution

The dimensionless coefficients A_f^n are not constants, but depend logarithmically on Q^2, the renormalization point of the operator product expansion. The operator rescaling and mixing analysis [11,12] for the twist-two flavor nonsinglet and singlet operators gives the renormalization group equations for the corresponding moments of the structure functions. In the context of the present path-integral formulation of OPE, the nonsinglet coefficients A_f^n and the nonsinglet moments only have contributions from the CI [Fig. 3(a) or Fig. 3(b)], since their DI contributions cancel among different flavors. On the other hand, the singlet coefficients A_f^n and the singlet moments have both the CI and DI [Fig. 3(c)] contributions. Therefore, it is possible to go to the single flavor basis and classify the equations in terms of CI and DI. For the CI which involves only the valence flavors (e.g., u and d for the nucleon), the renormalization equation is

$$\frac{d}{d\ln Q^2}M_f^n(\mathrm{CI})=\frac{\alpha_s(Q^2)}{8\pi}a_{qq}^n M_f^n(\mathrm{CI}), \tag{30}$$

where a_{qq}^n is the anomalous dimension coefficient. For the DI the equation is

$$\frac{d}{d\ln Q^2}M_f^n(\mathrm{DI})=\frac{\alpha_s(Q^2)}{8\pi}\left(a_{qq}^n M_f^n(\mathrm{DI}) + \frac{1+(-)^n}{2}a_{qG}^n M_G^n\right), \tag{31}$$

where a_{qG}^n is the anomalous dimension coefficient for operator mixing with the gluon operators and M_G^n is the moment for the gluon distribution function. We note that this mixing with gluon operators only contributes to $n=even$. As we can see, Eq. (31) involves the DS parton only.

We should stress that in the literature [13,16,17] the nonsinglet case has frequently been identified with valence. This is clearly incorrect. As we see from Eq. (26) that $A_f^{n=even}(\mathrm{CI})$ includes the CS partons in addition to the valence partons. Detailed study of this subject on the lattice has been carried out for the matrix elements and form factors of the nucleon from the three-point functions as well as hadron masses from the two-point functions [4]. It is shown when the CS quarks are removed by prohibiting pair-production through the Z graphs in the CI, the hadron structure and masses are greatly affected. It is learned that the CS quarks are responsible for the meson dominance in the form factors, the deviation of F_A/D_A and F_S/D_S from the nonrelativistic $SU(6)$ limit, the hyperfine splittings, and the constituent quark masses [4]. In the context of the parton model, they are responsible for the difference between $\overline{u}(x)$ and $\overline{d}(x)$ in the proton.

Following Altarelli and Parisi [13], the rescaling and mixing equations in Eqs. (30) and (31) can be translated into integral-differential equations which are the evolution equations for the parton densities. Therefore, for the CI the evolution equation for the unpolarized valence and CS partons is

$$\frac{dq_{v+cs}(x,Q^2)}{d\ln Q^2}=\frac{\alpha_s(Q^2)}{2\pi}\int_x^1\frac{dy}{y}P_{qq}\left(\frac{x}{y}\right)q_{v+cs}(y,Q^2), \tag{32}$$

where

$$\int_0^1 d\,z z^{n-1}P_{qq}(z)=\frac{a_{qq}^n}{4}. \tag{33}$$

For the CS antiparton density, the equation is similar

$$\frac{d\,\overline{q}_{cs}(x,Q^2)}{d\ln Q^2}=\frac{\alpha_s(Q^2)}{2\pi}\int_x^1\frac{dy}{y}P_{qq}\left(\frac{x}{y}\right)\overline{q}_{cs}(y,Q^2). \tag{34}$$

For the DS partons in the DI [Fig. 1(c)], the evolution equations from Eq. (31) are

$$\frac{d(q_{ds}+\overline{q}_{ds})(x,Q^2)}{d\ln Q^2}=\frac{\alpha_s(Q^2)}{2\pi}\int_x^1\frac{dy}{y}\left[P_{qq}\left(\frac{x}{y}\right)(q_{ds}+\overline{q}_{ds})\times(y,Q^2)+P_{qG}\left(\frac{x}{y}\right)G(y,Q^2)\right], \tag{35}$$

$$\frac{d(q_{ds}-\overline{q}_{ds})(x,Q^2)}{d\ln Q^2}=\frac{\alpha_s(Q^2)}{2\pi}\int_x^1\frac{dy}{y}P_{qq}\left(\frac{x}{y}\right)\times(q_{ds}-\overline{q}_{ds})(y,Q^2), \tag{36}$$

where

$$\int_0^1 d\,z z^{n-1}P_{qG}(z)=\frac{a_{qG}^n}{4}, \tag{37}$$

and $G(y,Q^2)$ is the unpolarized gluon distribution function.

Finally, the gluon evolution equation is

$$\frac{dG(x,Q^2)}{d\ln Q^2}=\frac{\alpha_s(Q^2)}{2\pi}\int_x^1\frac{dy}{y}\left\{P_{Gq}\left(\frac{x}{y}\right)\times\left[\sum_{f=val.fla.}(q_{v+cs}^f+\overline{q}_{cs}^f)(y,Q^2)+\sum_{f=DSfla.}(q_{ds}^f+\overline{q}_{ds}^f)(y,Q^2)\right]+P_{GG}\left(\frac{x}{y}\right)G(y,Q^2)\right\}. \tag{38}$$

It appears that, except for the gluon distribution, the evolution equations derived above are different from the Dokshitzer-Gribov-Lipatov-Altarelli-Parisi (DGLAP) evolution equations in the manner of Dokshitzer [14], Gribov and Lipatov [15], and Altarelli and Parisi [13] due to an extra CS degree of freedom in Eq. (34) which evolves like the valence in Eq. (32). However, since the evolution equations are linear in the parton distribution functions, once one defines the total sea to be the sum of CS and DS, i.e.,

$$q_s(x,Q^2)\equiv q_{cs}(x,Q^2)+q_{ds}(x,Q^2),$$
$$\overline{q}_s(x,Q^2)\equiv\overline{q}_{cs}(x,Q^2)+\overline{q}_{ds}(x,Q^2), \tag{39}$$

the sum of twice of Eq. (34) and Eq. (35) becomes

$$\frac{d(q_s+\overline{q}_s)(x,Q^2)}{d\ln Q^2}=\frac{\alpha_s(Q^2)}{2\pi}\int_x^1\frac{dy}{y}\left[P_{qq}\left(\frac{x}{y}\right)(q_s+\overline{q}_s)(y,Q^2)+P_{qG}\left(\frac{x}{y}\right)G(y,Q^2)\right]. \tag{40}$$

This is exactly the evolution of sea partons in the DGLAP equation. Similarly, the difference between Eq. (32) and Eq. (34) leads to the evolution of the valence partons in the DGLAP equation,

$$\frac{dq_v(x,Q^2)}{d\ln Q^2}=\frac{\alpha_s(Q^2)}{2\pi}\int_x^1\frac{dy}{y}P_{qq}\left(\frac{x}{y}\right)q_v(y,Q^2). \tag{41}$$

Thus, we see DGLAP equations can be derived from the path-integral formalism. However, the present form with the separation of CS from the DS offers a separate evolution of the CS in Eq. (34) which are decoupled from the valence, the DS, and the gluon. This decoupling is retained when higher orders are considered [18]. This affords the possibility of maintaining the separation of the CS and DS parton distributions when they are fitted to experiments at certain Q_0^2 and evolved up or down in Q^2. This is consistent with the classification into valence, CS, and DS in Fig. 1 and Eqs. (6) and (9) at all Q^2 from the path-integral formalism in the first place. Although, at leading twists, it makes no difference whether one considers the separate evolutions of CS and DS in Eqs. (34) and (35) or the combined evolution in Eq. (40), it may be necessary to consider the separate evolutions of CS and DS when higher twists are taken into account [19].

IV. PHENOMENOLOGICAL CONSEQUENCES

After the dynamical parton degrees of freedom are classified as valence, connected sea (CS), and disconnected sea (DS) via the path-integral diagrams in Fig. 1, one may question if there is an advantage to separating the CS from the DS. After all, both the CS and DS are pair-produced sea, only with different topology in the path-integral diagrams. In the previous section, we have shown that the CS parton evolves the same way as the valence, i.e. it is decoupled from the DS and the gluons in the evolution equation. This is consistent with the classification of the parton degrees of freedom into valence, CS, and DS at all Q^2. In the following, we shall show that it is useful to distinguish CS from DS because they have different small x behaviors. This is especially important in view of the fact that, in the nucleon, $\overline{u}$ and $\overline{d}$ have both the CS and DS parts, yet $\overline{s}$ has only the DS part. We further note that the Gottfried sum rule violation is attributable to the CS partons primarily. We finally assess the magnitude of the momentum fraction due to the CS and DS partons.

A. Small x behavior

Since the CS parton is in the connected insertion which is flavor nonsinglet like the valence, its small x behavior reflects the leading Reggeon exchanges of $\rho,\omega,a_2\ldots$ and thus should be like $x^{-1/2}$ [20–23]. On the other hand, the DS is flavor singlet and can have Pomeron exchanges, its small x behavior goes like x^{-1} [20–22]. Therefore, we have

$$\overline{u}_{cs}/\overline{d}_{cs}(x,Q_0^2) \underset{x\to 0}{\sim} x^{-1/2}, \tag{42}$$

$$\overline{u}_{ds}(x,Q_0^2)\sim\overline{d}_{ds}(x,Q_0^2)\sim\overline{s}(x,Q_0^2) \underset{x\to 0}{\sim} x^{-1} \tag{43}$$

at certain Q_0. As a result,

$$\overline{u}(x,Q_0^2)-\overline{d}(x,Q_0^2) \underset{x\to 0}{\sim} x^{-1/2}, \tag{44}$$

and this has been incorporated in the fitting of experimental results at some input scale Q_0^2 [24–26]. On the other hand, it has been taken for granted that $\overline{u}(x,Q_0^2)+\overline{d}(x,Q_0^2)$ has the same behavior as $\overline{s}(x,Q_0^2)$ in the fitting of the experiments. In other words, it is assumed that

$$\frac{1}{2}[\overline{u}(x,Q_0^2)+\overline{d}(x,Q_0^2)]\sim 2\overline{s}(x,Q_0^2), \tag{45}$$

in the fitting of parton distributions at $Q_0^2=1.6$ GeV^2 for CTEQ4 [24] and $Q_0^2=1$ GeV^2 for Martin, Roberts, Stirling, and Thorne (MRST) [26]. This has made the assumption that both the $\overline{u},\overline{d}$, like $\overline{s}$, have only the DS component. We proved in Sec. II [Eqs. (6) and (9)] that this is not true and that $\overline{u}$ and $\overline{d}$ have CS in addition to DS. Therefore, the correct parametrization for $\frac{1}{2}[\overline{u}(x,Q_0^2)+\overline{d}(x,Q_0^2)]$ should be

$$\frac{1}{2}[\overline{u}(x,Q_0^2)+\overline{d}(x,Q_0^2)]=A\overline{s}(x,Q_0^2)+\frac{1}{2}[\overline{u}_{cs}(x,Q_0^2)+\overline{d}_{cs}(x,Q_0^2)], \tag{46}$$

where A is a proportional constant. In the $SU(3)$ flavor symmetric limit, $A=1$. The second term on the right hand side of Eq. (46) is the CS part and has the $x^{-1/2}$ small x behavior. As far as we know, this kind of parametrization for $\frac{1}{2}[\overline{u}(x,Q_0^2)+\overline{d}(x,Q_0^2)]$ has not been taken into account in extracting the parton distribution functions. When this CS degree of freedom is incorporated in the sum of $\overline{u}$ and $\overline{d}$ in addition to the difference, we will have a different result from the present global analyses which will lead to different predictions on the parton distributions at high Q^2 relevant to LHC.

B. Origin of Gottfried sum rule violation

The NMC experiments of the F_2 structure functions of the proton and deuteron [2] reveal that the Gottfried sum rule

$$S_G=\int_0^1 dx\,\frac{F_2^p(x)-F_2^n(x)}{x}=\frac{1}{3}, \tag{47}$$

is violated due to fact that $\overline{u}\neq\overline{d}$ in the proton. This is verified in the Drell-Yan experiment E866/NuSea [27]. It has been shown [3] that the DS partons in Fig. 1(c) cannot give rise to a different $\overline{u}$ and $\overline{d}$ when $m_u=m_d$. It is noted that in Fig. 1(c) the flavor indices in the quark loop are separately traced from those in the propagators associated with the nucleon interpolation field, only the latter reflects the valence nature of the proton. Hence, Fig. 1(c) does not distinguish a loop with an u quark from that with a d quark at the flavor symmetric limit, i.e., $m_u=m_d$. In other words, $\overline{u}_{ds}(x,Q^2)=\overline{d}_{ds}(x,Q^2)$. On the other hand, the origin of $\overline{u}(x,Q^2)\neq\overline{d}(x,Q^2)$ can come from the CS antipartons in Fig. 1(b). Thus, the violation of the Gottfried sum rule originates entirely from the CS partons in the charge symmetric limit: i.e.,

$$\int_0^1 dx\,\frac{F_2^p(x,Q^2)-F_2^n(x,Q^2)}{x}=\frac{1}{3}+\frac{2}{3}\int dx[\overline{u}_{cs}(x,Q^2)-\overline{d}_{cs}(x,Q^2)]. \tag{48}$$

We shall see later that to $O(\alpha_s)$ and $O(1/Q^2)$, this turns out to be a sum rule.

Due to the fact that

$$\int_0^1 dx P_{qq}(x)=\frac{a_{qq}^1}{4}=0, \tag{49}$$

where a_{qq}^1 is the anomalous dimension coefficient in Eq. (33), Eqs. (41) and (34) lead to

$$\frac{d}{d\ln Q^2}\int_0^1 dx\,q_v(x,Q^2)=0, \tag{50}$$

$$\frac{d}{d\ln Q^2}\int_0^1 dx\,\overline{q}_{cs}(x,Q^2)=0. \tag{51}$$

We see that the CS antiparton number, like the valence number, is conserved, i.e., independent of Q^2. This is in contrast with the DS partons whose number is not conserved due to the pair-creation from the gluon. However, the conservation of the CS antiparton number is only good in the leading logarithmic approximation, i.e., good to $O(\alpha_s)$ and $O(1/Q^2)$. Whereas, the conservation of the vector current protects the charges, thus the valence quark number, against any Q^2 correction [11–13].

We note that the sum in Eq. (48) is in terms of the CS antipartons numbers. Thus to leading logarithmic approximation, it is a sum rule

$$\int_0^1 dx\,\frac{F_2^p(x)-F_2^n(x)}{x}=\frac{1}{3}+\frac{2}{3}[n_{\overline{u}_{cs}}-n_{\overline{d}_{cs}}], \tag{52}$$

where $n_{\overline{u}_{cs}}/n_{\overline{d}_{cs}}$ is the $\overline{u}_{cs}/\overline{d}_{cs}$ number.

C. Magnitude of the connected sea partons

We do not know precisely how large the magnitude of the CS partons and antipartons are in comparison with those of the valence and the DS unless one fits the DIS and Drell-Yan experiments with an explicit separation of the CS and the DS. But there are hints which are helpful in this respect. From the New Muon Collaboration (NMC) experiments on the F_2 structure function of the proton and deuteron [2], the sum in Eq. (52) is measured to be 0.235 ± 0.026 at $Q^2 = 4$ GeV^2, significantly smaller than the Gottfried sum rule prediction of 0.333. This implies that

$$n_{\bar{u}_{cs}} - n_{\bar{d}_{cs}} = \int_0^1 dx [\bar{u}_{cs}(x,Q^2) - \bar{d}_{cs}(x,Q^2)] = -0.147 \pm 0.039, \quad (53)$$

at $Q^2 = 4$ GeV^2 which is not negligible compared with the valence numbers of u and d.

Since $\bar{u}$ (similarly $\bar{d}$) has contributions from the CS and DS, i.e., $\bar{u}(x) = \bar{u}_{cs}(x) + \bar{u}_{ds}(x)$ and $\bar{s}$ is from the DS only, one expects that

$$\langle x \rangle_{\bar{u}} = \langle x \rangle_{\bar{u}_{cs}} + \langle x \rangle_{\bar{u}_{ds}} > \langle x \rangle_{\bar{s}}. \quad (54)$$

Indeed, in the CCFR dimuon data, $\bar{s}$ is about 50% of $(\bar{u} + \bar{d})/2$ at $Q^2 \simeq 4$ GeV^2 in the range of x between 0.01 and 0.20. Since $\bar{u} - \bar{d}$, which only has the CS contribution, also peaks in this x range, we think the observed difference between $(\bar{u} + \bar{d})/2$ and $\bar{s}$ is mainly duw to the CS part of $(\bar{u} + \bar{d})/2$. As a result, one expects that the momentum fraction of the CS part of $(\bar{u} + \bar{d})/2$ is comparable to that of the DS part, i.e.,

$$\frac{1}{2}(\langle x \rangle_{\bar{u}_{cs}} + \langle x \rangle_{\bar{d}_{cs}}) \sim \frac{1}{2}(\langle x \rangle_{\bar{u}_{ds}} + \langle x \rangle_{\bar{d}_{ds}}) \sim \langle x \rangle_{\bar{s}}, \quad (55)$$

at $Q^2 = 4$ GeV^2. Any experiment which measures $(\bar{u} + \bar{d})/2$ and $\bar{s}$ at very small x, e.g., $10^{-3} - 10^{-4}$ will be very useful in verifying the form of the distribution function prescribed in Eq. (46).

V. CONCLUSION

In conclusion, we have formulated the hadronic tensor $W_{\mu\nu}$ of the deep inelastic scattering starting from the Euclidean path-integral formalism. We found that it can be divided into three gauge-invariant and topologically distinct parts which we classify as the valence-connected sea partons, the connected sea antipartons and the disconnected-sea partons and antipartons. This admits a separation of the CI from the DI and the partons from the antipartons. Since the CS is in the CI and the DS in the DI, they have different small x behaviors. We show that the operator product expansion is simply a short distance Taylor expansion of functions in the path integral. From operator rescaling and mixing, we derive the evolution equations which show that the CS partons evolve like the valence and their numbers are conserved in the leading log approximation. We stress that in the nucleon $\bar{u}$ and $\bar{d}$ partons have both the connected and disconnected sea contributions, whereas, $\bar{s}$ partons have only the disconnected sea contribution. A global analysis of the experimental data is needed to take this difference into account to fit the parton distribution functions.

ACKNOWLEDGMENTS

This work is partially supported by U.S. DOE Grant No. DE-FG05-84ER40154. The author would like to thank S. Brodsky, N. Christ, G. T. Garvey, X. Guo, X. Ji, L. Mankiewicz, R. McKeown, C. S. Lam, G. Martinelli, J. C. Peng, J. Qiu, W. K. Tung, and C. P. Yuan for useful discussions.

[1] European Muon Collaboration, J. Ashman *et al.*, Phys. Lett. B **206**, 364 (1988); E143 Collaboration, K. Abe *et al.*, Phys. Rev. Lett. **74**, 346 (1995); SMC, D. Adams *et al.*, Phys. Rev. D **56**, 5330 (1997).
[2] NMC, P. Amaudruz *et al.*, Phys. Rev. Lett. **66**, 2712 (1991); M. Arneodo *et al.*, Phys. Rev. D **50**, R1 (1994).
[3] K. F. Liu and S. J. Dong, Phys. Rev. Lett. **72**, 1790 (1994).
[4] K. F. Liu, S. J. Dong, T. Draper, D. Leinweber, J. Sloan, W. Wilcox, and R. M. Woloshyn, Phys. Rev. D **59**, 112001 (1999).
[5] W. Wilcox, Nucl. Phys. B (Proc. Suppl.) **B30**, 491 (1993).
[6] This point was brought up by R. Jaffe during the Gordon Conference on Nuclear Physics and QCD in 1999.
[7] See, for example, S. Adler and R. Dashen, *Current Algebra and Applications to Particle Physics* (Benjamin, New York, 1968), p. 254.
[8] We shall follow the derivation of operator analysis in M. E. Peskin and D. V. Schroeder, *Quantum Field Theory* (Addison-Wesley, Reading, MA, 1995).
[9] G. Martinelli and C. T. Sachrajda, Nucl. Phys. **B316**, 355 (1989).
[10] M. Göckeler *et al.*, Phys. Rev. D **53**, 2317 (1996).
[11] H. Georgi and H. D. Politzer, Phys. Rev. D **9**, 416 (1974).
[12] D. Gross and F. Wilczek, Phys. Rev. D **9**, 980 (1974).
[13] G. Altarelli and G. Parisi, Nucl. Phys. **B126**, 298 (1977).
[14] Yu. Dokshitzer, Zh. Éksp. Teor. Fiz. **73**, 1216 (1977) [Sov. Phys. JETP **46**, 641 (1977)].
[15] V. N. Gribov and L. N. Lipatov, Yad. Fiz. **15**, 781 (1972) [Sov. J. Nucl. Phys. **15**, 438 (1972)]; **15**, 1218 (1972) [**15**, 675 (1972)].
[16] J. C. Collins and J. Qiu, Phys. Rev. D **39**, 1398 (1989).
[17] E. Eichten *et al.*, Rev. Mod. Phys. **56**, 579 (1984).
[18] W. Furmanski and R. Petronzio, Z. Phys. C **11**, 293 (1982).
[19] X. Guo and J. Qiu (private communication).
[20] J. Kuti and V. F. Weissopf, Phys. Rev. D **4**, 3418 (1971).
[21] J. W. Moffat, *Schladming Lectures 1972* [Acta Phys. Austriaca, Suppl. **IX**, 605 (1972)].

[22] E. Reya, Phys. Rep. **69**, 195 (1981).
[23] S. Brodsky and I. Schmidt, Phys. Rev. D **43**, 179 (1991).
[24] H. L. Lai *et al.*, Phys. Rev. D **55**, 1280 (1997).
[25] H. L. Lai *et al.*, Eur. Phys. J. C **12**, 375 (2000).
[26] A. D. Martin, R. G. Roberts, W. J. Stirling, and R. S. Thorne, Eur. Phys. J. C **4**, 463 (1998).
[27] E866/NuSea Collaboration, J. C. Peng *et al.*, Phys. Rev. D **58**, 092004 (1998).